IJC Heart & Vasculature 38 (2022) 100938

Contents lists available at ScienceDirect

IJC Heart & Vasculature

journal homepage: www.sciencedirect.com/journal/ijc-heart-and-vasculature

Relationship between lung injury extent and phenotype manifested in non-contrast CT and cardiac injury during acute stage of COVID-19

Aaron So [a,b,1], Zehong Yang [c,1], Liang Li [d], Wang Li [e], Cheng Pan [h], Prushoth Vivekanantha [b], Hye Won Yun [b], Xin Yue Xie [b], Chun-Ho Yun [f], Wei-Ming Huang [f], Chung-Lieh Hung [g], Ming Gao [c], Xiang Zhang [c], Yunfei Zha [e,*], Jun Shen [c,*]

[a] Imaging Program, Lawson Health Research Institute, London, Ontario, Canada
[b] Department of Medical Biophysics, Schulich School of Medicine and Dentistry, Western University, London, Ontario, Canada
[c] Department of Radiology, Sun Yat-Sen Memorial Hospital, Sun Yat-Sen University, Guangzhou, Guangdong, China
[d] Department of Radiology, Renmin Hospital of Wuhan University, Wuhan, Hubei, China
[e] Department of Infection Prevention and Control Office, Renmin Hospital of Wuhan University, Wuhan, Hubei, China
[f] Department of Radiology, Mackay Memorial Hospital, Taipei, Taiwan
[g] Department of Cardiology, Mackay Memorial Hospital, Taipei, Taiwan
[h] Critical Care, London Health Sciences Centre, London, Ontario, Canada

ARTICLE INFO

Keywords:
COVID-19
SARS-CoV-2
Acute cardiac injury
Non-contrast computed tomography (NCCT)
Inflammation

ABSTRACT

Purpose: This study evaluated the diagnostic values of the extent of lung injury manifested in non-contrast enhanced CT (NCCT) images, the inflammatory and immunological biomarkers C-reactive protein (CRP) and lymphocyte for detecting acute cardiac injury (ACI) in patients with COVID-19. The correlations between the NCCT-derived parameters and arterial blood oxygen level were also investigated.
Methods: NCCT lung images and blood tests were obtained in 143 patients with COVID-19 in approximately two weeks after symptom onset, and arterial blood gas measurement was also acquired in 113 (79%) patients. The diagnostic values of normal, moderately and severely abnormal lung parenchyma volume relative to the whole lungs (RVNP, RVMAP, RVSAP, respectively) measured from NCCT images for detecting the heart injury confirmed with high-sensitivity troponin I assay was determined.
Results: RVNP, RVMAP and RVSAP exhibited similar accuracy for detecting ACI in COVID-19 patients. RVNP was significantly lower while both RVMAP and RVSAP were significantly higher in the patients with ACI. All of the NCCT-derived parameters exhibited poor linear and non-linear correlations with P_aO_2 and S_aO_2. The patients with ACI had a significantly higher CRP level but a lower lymphocyte level compared to the patients without ACI. Combining one of these two biomarkers with any of the three NCCT-derived parameter further improved the accuracy for predicting ACI in patients with COVID-19.
Conclusion: The NCCT-delineated normal and abnormal lung parenchmyma tissues were statistically significant predictors of ACI in patients with COVID-19, but both exhibited poor correlations with the arterial blood oxygen level. The incremental diagnostic values of lymphocyte and CRP suggested viral infection and inflammation were closely related to the heart injury during the acute stage of COVID-19.

1. Introduction

The coronavirus disease 2019 (COVID-19) is caused by the severe acute respiratory syndrome coronavirus 2 (SARS-CoV-2). This ongoing pandemic continues to impact our daily lives in many ways. One potential complication in patients contracted SARS-CoV-2 is acute cardiac injury (ACI)[1,2]. While COVID-19 is commonly diagnosed with a polymerase chain reaction (PCR) test and a non-contrast computed tomography (NCCT) chest scan, the more specific functional cardiac imaging or high-sensitivity troponin I (hs-TnI) assay is not frequently acquired to assess the potential cardiac injury associated with COVID-19. The exact pathway leading to the cardiac damage in some COVID-

* Corresponding authors.
E-mail addresses: zhayunfei999@126.com (Y. Zha), shenjun@mail.sysu.edu.cn (J. Shen).
[1] These authors are co-first authors.

https://doi.org/10.1016/j.ijcha.2021.100938
Received 28 January 2021; Received in revised form 28 November 2021; Accepted 21 December 2021
Available online 25 December 2021

19 positivie patients has not been fully elucidated, despite the proposal of several possible mechanisms[3–6]. Knowledge of the underlying pathophysiology of cardiac injury associated with COVID-19 would be useful to inform appropriate treatments to minimize cardiac injury and mortality[7,8], particularly during the early phase of viral contraction. The primary objective of this study was to investigate the diagnostic value of NCCT for detecting ACI during the early stage of COVID-19. The finding would inform whether NCCT is useful to determine the likelihood of ACI in situations where functional cardiac imaging and hs-TnI are not available during the initial diagnostic procedure. The secondary objective was to determine the correlation between the extent of lung injury delineated with NCCT and the arterial blood oxygen level, from which the potential cause of the heart damage could be postulated.

2. Methods

2.1. COVID-19 patients

The findings of the NCCT test and blood test of 143 Chinese patients (55.14 ± 13.72 years old; 69 male and 74 female) who were admitted to the Renmin Hospital, Wuhan University (Wuhan, Hubei, China), from January to March 2020 were retrospectively analyzed. The study was approved by the institution ethics review board. The average time interval between symptom onset and hospitalization was 14.26 ± 0.75 days (mean $\pm$ standard error). The average time interval between the NCCT scan and blood test was 1.83 ± 0.40 days. The average time interval between the NCCT scan and PCR test was 2.84 ± 0.30 days. All the 143 COVID-19 patients (including 113 with and 30 without arterial blood gas measurement) were classified into two study groups according to their troponin-I levels: patients without ACI whose troponin-I was less than or equal to 2 ng/L[9,10], and patients with ACI whose troponin-I was greater than 2 ng/L. All the NCCT chest scans were performed with a Siemens Somatom Spirit CT scanner (Siemens Healthineers, Erlangen, Germany) with the following acquisition settings: 130 kV tube voltage, 92 mA tube current, 1.0 s gantry rotation period, 5 mm tomographic slice thickness. Each blood test included the measurement of lactate dehydrogenase (LDH) which is a marker of tissue damage[11], white blood cell (WBC), neutrophil, lymphocyte, C-reactive protein (CRP) which is a marker of inflammation[13], and troponin-I which is an enzyme and specific marker of cardiac injury[9]. The patients who received the arterial blood gas measurements were not mechanically ventilated or supplied with supplementary oxygen when the measurements were acquired.

2.2. Analysis of NCCT chest images of COVID-19 patients

Analysis of NCCT chest images was performed with the Analyze 14.0 software (AnalyzeDirect Inc., Overland Park, Kansas). From each set of NCCT images, the left and right lungs across all tomographic slices were delineated with the automatic contour detection function in Analyze. The detected contour of each lung was then modified manually if needed to minimize the coverage of the trachea, bronchi and large pulmonary blood vessels. Thereafter, the CT number in each voxel in each delineated lung region and the corresponding image voxel dimensions (length, width and depth) were exported using the histogram function in Analyze. Next, the volume of each lung was calculated as the number of image voxel covering the lung multiplied by the image voxel dimensions.

Normal lung parenchyma was defined as the image voxel within the lungs that had a CT number between −950 and −700 HU. Abnormal lung parenchyma was further classified into two categories according to their differences in tissue characteristics[12]: moderately abnormal parenchyma, which had a low elastance (high compliance) and manifested as ground glass opacification, had a mean CT number between −600 to −150 HU; severely abnormal parenchyma, which had a high elastance (low compliance) and manifested as consolidation, had a mean CT number between −149 to 150 HU (Fig. 1). The relative volume of normal lung parenchyma (RVNP), moderately abnormal lung parenchyma (RVMAP) and severely abnormal lung parenchyma (RVSAP) with respect to the total lung volume (sum of the left and right lung volumes) were calculated accordingly.

2.3. Estimation of decrease in normal lung parenchyma in COVID-19 patients

To estimate the magnitude of RVNP reduction from baseline in the COVID-19 patients, the CT images of 32 Chinese patients who did not contract SARS-CoV-2 were used as the control subjects for comparison. These images were acquired at MacKay Memorial Hospital in Taipei, Taiwan, between 2010 and 2012 for perfusion assessment as part of the diagnostic procedure. Only the images acquired at the initial non-contrast phase were used for analysis to ensure the image voxel intensity in the lung parenchyma tissue was unaffected by the administration of contrast solution. These patients were selected as the control subjects for comparison since their race and mean age matched to those of the COVID-19 patients. The control patients reported to never smoke (not ex-smoker nor smoker at the time of imaging test), had no known lung diseases and diabetes (to avoid the effect of microvascular diseases). Furthermore, the non-contrast CT images of the control patients showed no sign of tumor and pneumonia in the lung region. These images were acquired a Siemens Definition Flash scanner with a tube voltage of 100 kV. A previous study showed that the CT numbers of the materials that are not highly-attenuating to X-rays (such as water and soft tissue) are minimally affected by the tube voltage settings.[25] The mean RVNP of the 32 control (non-COVID-19) subjects was estimated from the middle eight centimeters of the left lung with the same Housfield Unit threshold (-950 to −700 HU) as for the COVID-19 patients. A previous post-mortem study showed that the average alveoli density in the middle section of the lung was a good representation of the average alveoli density of the whole lung.[26]

2.4. Data and statistical analysis

All statistical analyses were performed with the SPSS software version 27 (IBM, Armonk, New York) and R Programming Language (version 3.0.1; http://www.Rproject.org). Any difference with a P value < 0.05 (two-tailed) was defined as statistically significant. All reported values were expressed as mean $\pm$ standard error. Logistic regression analysis was performed to determine if RVNP, RVMAP, RVSAP, C-reactive protein (CRP), lymphocyte-to-CRP (L-C) ratio, or a combination of CRP or L-C ratio with any of the NCCT-derived parameters (RVNP, RVMAP or RVSAP) was a statistically significant predictor of ACI. The optimal threshold of each significant predictor for differentiating between the ACI and non-ACI cases was determined from the Youden index, from which the sensitivity, specificity, positive predictive value, negative predictive value and accuracy of each significant predictor were calculated. The receiver operating characteristic (ROC) curve and ROC curve (AUC) of each predictor were also derived.

In each of the two study groups (patients with and without ACI), the mean levels of RVNP, RVMAP, RVSAP and CRP in the individuals who also had hypertension or diabetes were also compared with the individuals without hypertension or diabetes using a one-way ANOVA test.

3. Results

3.1. P_aO_2, S_aO_2, biomarker measurements in COVID-19 patients with and without ACI

Of the 113 COVID-19 patients who had the arterial blood gas measurement, 56 patients (60.80 ± 1.49 years old, 32 male and 24 female) had the arterial partial pressure of oxygen (P_aO_2) level below the normal

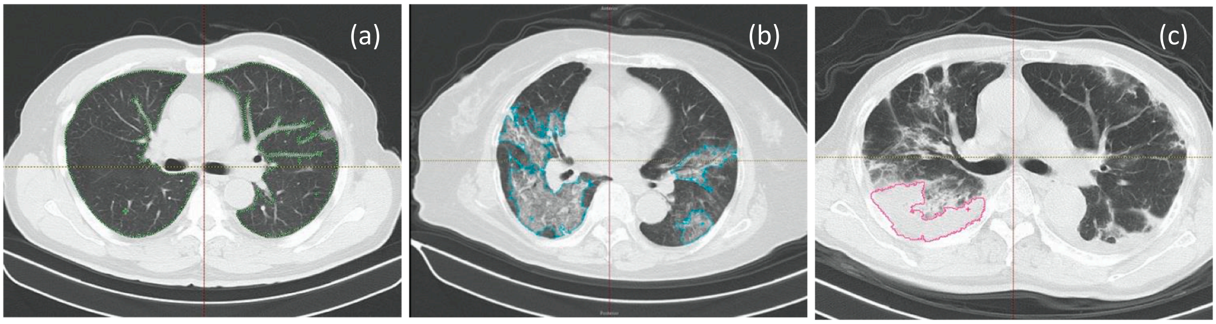

Fig. 1. Three ranges of CT number used to differentiate between different lung phenotypes observed in our COVID-19 patients: (a) normal parenchyma (−950 to −700 HU, green regions); (b) moderately abnormal parenchyma manifested as ground-glass opacification (−600 to −150 HU, light blue regions); (c) severely abnormal parenchyma manifested as consolidation (-149 to 150 HU, pink region).

range (10.6–13.3 kPa or 80–100 mmHg), and 57 patients (54.56 ± 1.88 years old, 30 male and 27 female) whose P_aO_2 was within the normal range. The mean P_aO_2 and arterial blood oxygen saturation (S_aO_2) levels were not statistically different between the patients with and without ACI ($p > 0.05$ between patient groups for both parameters). The recorded fraction of inspired oxygen (FiO_2) level in all the patients was 0.21 (21%), indicating that no supplemental oxygen was given to these patients. The mean troponin I level in the 66 patients without ACI (49.06 ± 13.43 years old, 26 M and 40F) was 0.80 ± 0.63 ng/L, which was statistically lower than the 2.0 ng/L threshold ($p < 0.05$). The mean troponin I level in the 77 patients with ACI (60.35 ± 11.66 years old, 43 M and 34F) was 10.87 ± 10.34 ng/L, which was statistically higher than the 2.0 ng/L threshold ($p < 0.05$) and the mean level in the patients without ACI ($p < 0.05$). The mean LDH level was also significantly higher in the patients with ACI ($p < 0.001$). The mean levels of the immunological and inflammatory biomarkers were also statistically different between the two patient groups ($p < 0.05$ for all the markers). The mean levels of P_aO_2, S_aO_2, WBC, neutrophil, lymphocyte, LDH, and troponin I for each study group (ACI versus no ACI) are summarized in Table 1 and Fig. 4.

Table 1
Comparison in the biomarkers and NCCT-derived relative normal and abnormal lung parenchyma volumes between COVID-19 patients with and without ACI.

	Absence of ACI	ACI	p value
Total number of patient	66	77	–
Age (mean ± SD, years)	49.06 ± 13.43	60.35 ± 11.66	< 0.001
Sex			
Female	40	34	–
Male	26	43	–
With Hypertension	10	19	–
With Diabetes	17	27	–
P_aO_2 (mmHg)	11.14 ± 2.98	10.85 ± 2.66	0.654
S_aO_2 (mmHg)	93.68 ± 9.10	95.53 ± 2.84	0.327
WBC ($\times10^9$/L)	5.19 ± 1.80	6.32 ± 2.97	0.006
Neutrophil ($\times10^9$/L)	3.25 ± 1.46	4.22 ± 2.22	0.003
Lymphocyte ($\times10^9$/L)	1.42 ± 0.61	1.03 ± 0.58	< 0.001
Troponin I (ng/L)	0.80 ± 0.63	10.87 ± 10.34	< 0.001
CRP (mg/L)	24.68 ± 38.04	62.40 ± 57.57	< 0.001
LDH (IU/L)	221.77 ± 67.16	327.04 ± 115.41	< 0.001
NCCT-derived lung injury metric (%)			
RVNP	71.50 ± 11.96	61.78 ± 12.73	< 0.001
RVMAP	12.78 ± 8.80	18.54 ± 9.68	< 0.001
RVSAP	1.43 ± 1.66	3.23 ± 3.27	< 0.001

Abbreviation: NCCT = Non-contrast chest computed tomography, ACI = Acute cardiac injury, WBC = White blood cells, RVNP = Relative volume of normal lung parenchyma, RVMAP = Relative volume of moderately abnormal lung parenchyma, RVSAP = Relative volume of severely abnormal lung parenchyma, CRP = C-reactive protein.

3.2. NCCT measurements in COVID-19 patients with and without ACI

In the 56 COVID-19 patients with compromised P_aO_2 (66.53 ± 1.80 mmHg), the RVNP with respect to the left lung volume, the right lung volume and the total lung volume was 62.63 ± 1.55%, 60.95 ± 1.70% and 59.01 ± 1.65%, respectively. There was no statistical difference in the RVNP between the left and right lungs for this patient group, indicating that the extent of lung injury was comparable between the two lungs. In the 57 COVID-19 patients with preserved P_aO_2 (97.81 ± 2.03 mmHg), the corresponding RVNP was 70.13 ± 1.56%, 70.06 ± 1.70% and 68.12 ± 1.72%, respectively. Similarly, there was no statistical difference in the RVNP between the left and right lungs for this patient group. In comparison, the mean RVNP of the control (non-COVID-19) subjects was estimated to be 81.85 ± 1.05%, which agreed with that reported in previous post-mortem studies.[26]

The Pearson's and Shearman's correlation coefficients between the RVNP and P_aO_2 in all the COVID-19 patients were 0.184 and 0.063 respectively. The Pearson's and Shearman's correlation coefficients between the RVNP and S_aO_2 were 0.065 and 0.029 respectively.

The RVMAP and RVSAP in the 56 patients with compromised P_aO_2 were 20.63 ± 1.27% and 3.53 ± 0.45% respectively, which were both statistically higher than those in the 57 patients with preserved P_aO_2 (14.68 ± 1.33% and 2.33 ± 0.36% respectively, $p < 0.05$ between patient groups for both variables). The Pearson's and Shearman's correlation coefficients between the RVMAP and P_aO_2 were −0.175 and 0.019 respectively, and between the RVMAP and S_aO_2 were −0.062 and 0.074 respectively. The Pearson's and Shearman's correlation coefficients between the RVSAP and P_aO_2 were −0.030 and 0.068 respectively, and between the RVSAP and S_aO_2 were −0.017 and 0.108 respectively. The scatter plots of P_aO_2 and S_aO_2 against RVNP, RVMAP and RVSAP are shown in Fig. 2.

The mean RVNP, RVMAP and RVSAP corresponding to the two COVID-19 patient groups (with and without ACI) are shown in Table 1. The RVNP in the COVID-19 patients with ACI was statistically lower than that in the patients without ACI ($p < 0.001$). In contrast, both the RVMAP and RVSAP in the COVID-19 patients with ACI were statistically higher than those in the patients without ACI ($p < 0.001$ between groups for both parameters).

3.3. Diagnostic values of NCCT, CRP and L-C ratio for detecting ACI in COVID-19 patients

Table 2 summarizes the diagnostic performance of RVNP, RVMAP, RVSAP, RVNP + CRP, RVMAP + CRP, and RVSAP + CRP. Logistic regression analysis revealed that each of RVNP, RVMAP, RVSAP and CRP had a moderate accuracy for detecting ACI in COVID-19 patients. The diagnostic accuracy improved when CRP was used in conjunction to RVNP, RVMAP or RVSAP as the predictor, with the combination of RSMAP and CRP yielded the highest accuracy (72%). The AUC of the

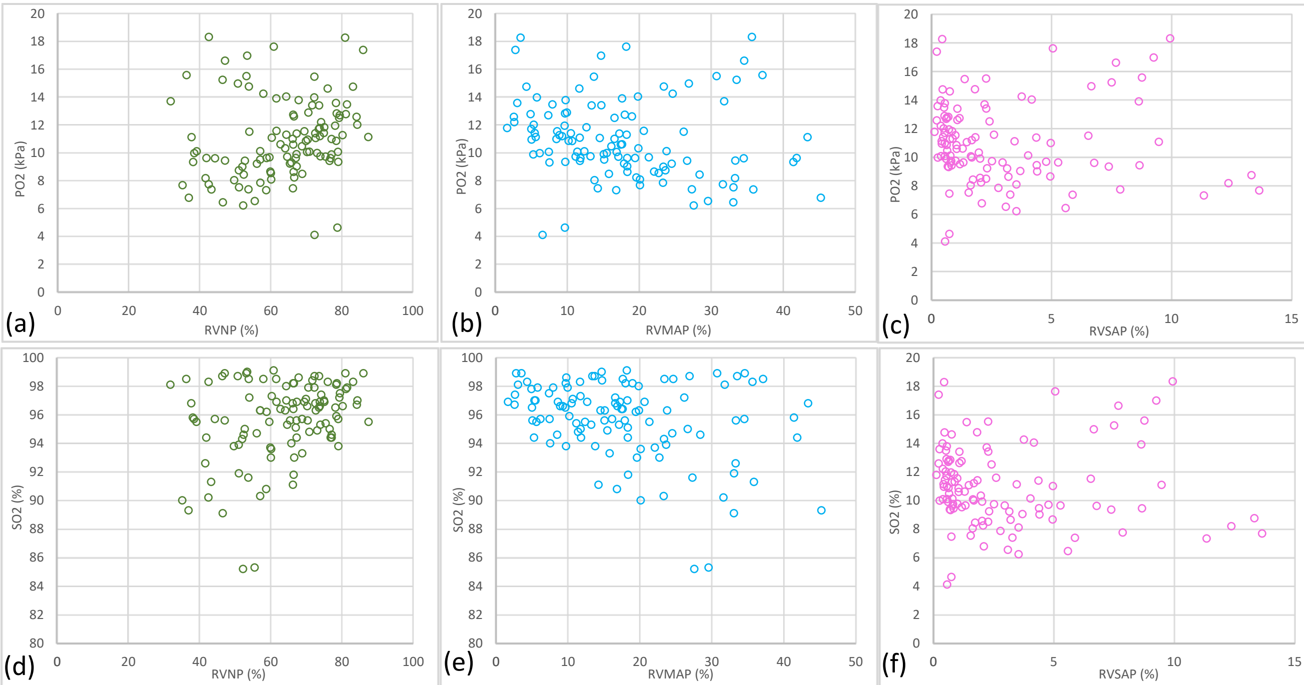

Fig. 2. Scatter plots of arterial partial oxygen pressure (P_aO_2) and blood oxygen saturation (S_aO_2) against relative volume of normal parenchyma (RVNP, a and d), relative volume of moderately abnormal parenchyma (RVMAP, b and e) and relative volume of severely abnormal parenchyma (RVSAP, c and f).

Table 2
Diagnostic performance of NCCT-derived normal and abnormal lung parenchyma volumes, CRP, and conjunctional use of these parameters for detecting ACI in COVID-19 patients.

NCCT	AUC	Accuracy(%)	Sensitivity (%)	Specificity (%)	PPV (%)	NPV (%)	p value
RVNP	0.73 (0.65, 0.82)	69.2 (61.0, 76.7)	66.2 (54.5, 76.4)	72.7 (60.2,82.6)	73.9 (61.7, 83.4)	64.9 (52.8, 75.4)	<0.001
RVMAP	0.70 (0.61, 0.78)	69.9 (61.7, 77.3)	74.0 (62.6, 83.0)	65.2 (52.3, 76.2)	71.2 (59.9, 80.5)	68.2 (55.2, 79.1)	<0.001
RVSAP	0.72 (0.64, 0.80)	69.2 (61.0,76.7)	81.8 (71.0, 89.4)	54.5 (41.9, 66.7)	67.7 (57.1, 76.8)	72.0 (57.3, 83.3)	<0.001
CRP	0.72 (0.64, 0.81)	67.8 (59.5, 75.4)	75.3 (54.0, 84.1)	59.1 (46.3, 70.8)	68.2 (57.1, 77.7)	67.2 (53.5, 78.6)	<0.001
LC ratio	0.74 (0.66, 0.82)	67.8 (59.5, 75.4)	53.2 (41.5, 64.7)	84.8 (73.9, 92.5)	80.4 (69.1, 88.3)	60.9 (54.6, 66.8)	<0.001
RVNP + CRP	0.75 (0.67, 0.83)	70.6 (62.4, 77.9)	77.9 (66.8, 86.3)	62.1 (49.3, 73.5)	70.6 (59.6, 79.7)	70.7 (57.1, 81.5)	<0.001
RVMAP + CRP	0.74 (0.66, 0.82)	72.0 (63.9, 79.2)	72.7 (61.2,82.0)	71.2 (58.6, 81.4)	74.7 (63.1, 83.7)	69.1 (56.6,79.4)	<0.001
RVSAP + CRP	0.75 (0.67, 0.83)	70.6 (62.4, 77.9)	71.4 (59.8, 80.9)	69.7 (57.0, 80.1)	73.3 (61.7, 82.6)	67.6 (55.1, 78.2)	<0.001
RVNP + LC ratio	0.74 (0.66, 0.82)	70.6 (62.4, 77.9)	70.1 (58.5, 79.8)	71.2 (58.6, 81.4)	74.0 (62.2, 83.2)	67.1 (54.8, 77.6)	<0.001
RVMAP + LC ratio	0.73 (0.64, 0.81)	72.0 (63.9, 79.2)	76.6 (65.3, 85.2)	66.7 (53.9, 77.5)	56.6 (48.1, 64.8)	72.8 (61.6, 81.8)	<0.001
RVSAP + LC ratio	0.74 (0.66, 0.82)	72.0 (63.9, 79.2)	84.4 (74.0, 91.3)	57.6 (44.8, 69.4)	69.9 (59.4, 78.7)	76.0 (61.5, 86.5)	<0.001

Abbreviation: NCCT = Non-contrast chest computed tomography, RVNP = Relative volume of normal lung parenchyma, RVMAP = Relative volume of moderately abnormal lung parenchyma, RVSAP = Relative volume of severely abnormal lung parenchyma, CRP = C-reactive protein, LC = lymphocyte-to-CRP, AUC = Area under the curve, PPV = Positive predictive value, NPV = Negative predictive value.

RVNP, RVMAP, RVSAP and CRP was 0.733, 0.698, 0.721 and 0.725 respectively. The corresponding AUC of the RVNP + CRP, RVMAP + CRP and RVSAP + CRP were 0.750, 0.743 and 0.754, respectively. When CRP was replaced by the lymphocyte-to-CRP (L-C) ratio as the conjunctional predictor, the overall diagnostic accuracy for detecting ACI did not improve further (Table 2 and Fig. 3).

4. Discussion

The primary objective of this retrospective study was to investigate the diagnostic values of NCCT-derived relative normal and abnormal lung parenchyma volumes for detecting ACI in COVID-19 patients within approximately two weeks of viral contraction. The secondary study objective was to investigate the correlation between the arterial blood oxygen level and the NCCT measurements in these patients, from which the potential mechanisms of cardiac injury during the acute phase of viral contraction could be speculated. Our findings revealed statistical differences in the mean RVNP, RVMAP and RVSAP between the patients without and with ACI. Furthermore, all of the RVNP, RVMAP and RVSAP were statistically significant predictors of ACI in the COVID-19 patients. When each of these NCCT-derived metrics was used conjunctionally with CRP or L-C ratio as the predictor, the corresponding diagnostic accuracy improved further. On the contrary, both the mean P_aO_2 and S_aO_2 levels were not statistically different between the patients without and with ACI. Additionally, both P_aO_2 and S_aO_2 exhibited a poor linear or non-linear correlation to all of the NCCT-derived parameters.

Several mechanisms have been proposed to explain the underlying mechanism of heart injury in the patients contracted SARS-coV-2.[3–6] The findings of this study suggested that viral infection was likely a main contributor of the heart injury during this stage of the disease, since the levels of both inflammatory (CRP) and immunological (WBC and neutrophil) markers were significantly higher in the ACI patient group. CRP is a type of protein synthesized by the hepatocytes in the liver, and elevation of the CRP level is a classic marker of systemic inflammation,[13,14] which is elicited by a cytokine storm as demonstrated in many patients with COVID-19.[15] A cytokine storm refers to an augmented immune reaction to tissue damage or infection, during which excessive pro-inflammatory cytokines are released into the blood in a short period

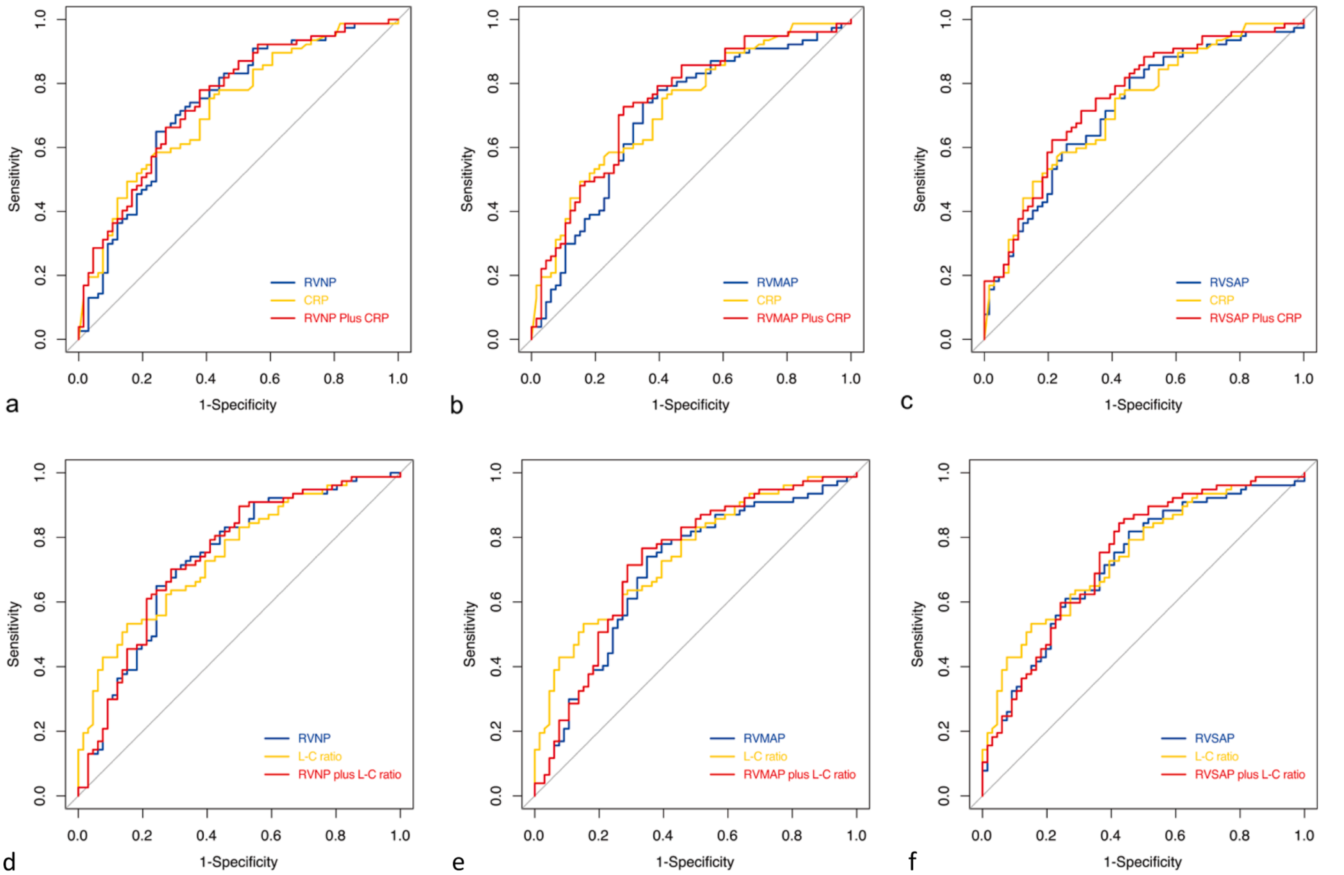

Fig. 3. Receiver operating characteristic (ROC) curve of different NCCT-derived parameters and serum biomarkers for detection of ACI in patients with COVID-19 at approximately two weeks after symptom onset: (a) RVNP, CRP and RVNP plus CRP; (b) RVMAP, CRP and RVMAP plus CRP; (c) RVSAP, CRP and RVSAP plus CRP; (d) RVNP, L-C ratio and RVNP plus L-C ratio; (e) RVMAP, L-C ratio and RVMAP plus L-C ratio; (f) RVSAP, L-C ratio and RVSAP plus L-C ratio. The area under the curve (AUC) corresponding to the parameters were RVNP 0.73 (95% CI: 0.65–0.82), RVMAP 0.70 (95% CI: 0.61–0.78), RVSAP 0.72 (95% CI: 0.64–0.80), CRP 0.72 (95% CI: 0.64–0.81), RVNP plus CRP 0.75 (95% CI: 0.67–0.83), RVMAP plus CRP 0.74 (95% CI: 0.66–0.82), RVSAP plus CRP 0.75 (95% CI: 0.67–0.83), L-C ratio 0.74 (95% CI: 0.66–0.82), RVNP plus L-C ratio 0.74 (95% CI: 0.66–0.82), RVMAP plus L-C ratio 0.73 (95% CI: 0.64–0.81), RVSAP plus L-C ratio 0.74 (95% CI: 0.66–0.82), respectively.

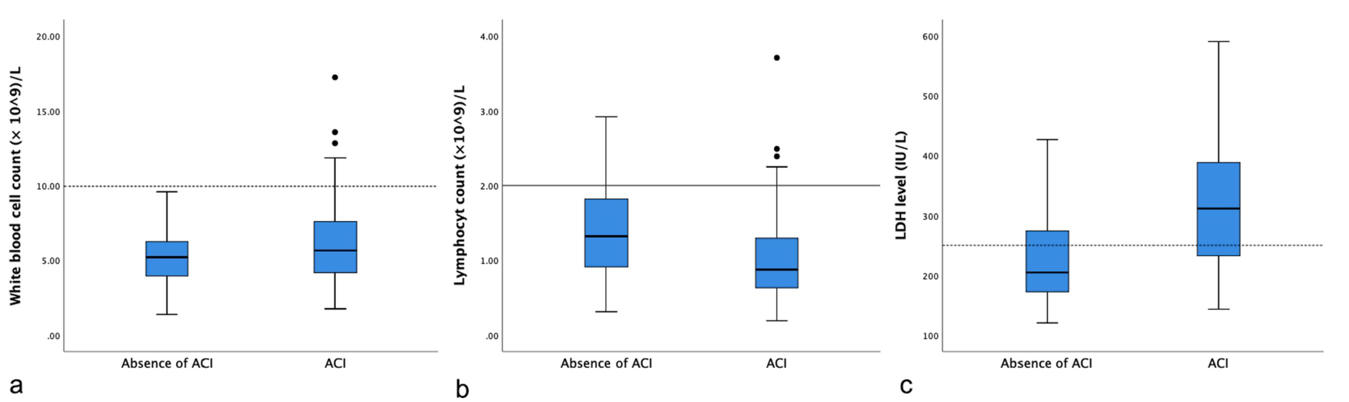

Fig. 4. Comparison in the number of (a) white blood cell, (b) lymphocyte and (c) lactate dehydrogenase (LDH) between the two COVID-19 patient groups (with and without ACI). The dashed line in each boxplot represents the respective upper limit of the normal range.

of time. Depending on its severity, a cytokine storm may lead to multi-organ damage and death.[16,17] Therefore, the magnitude of CRP level may have implications on organ damage as shown in this study. The CRP level is usually below 10 mg/L under normal condition.[18] A significant increase in the CRP level was observed in our patients with the level on average 20 to 60 mg/L, agreeing with the levels reported in previous studies on COVID-19 patients.[18] Furthermore, the average CRP level of the COVID-19 patients without ACI was more than 20 mg/L but less than the average levelsof the patients with ACI, suggesting a threshold level of CRP might exist below which myocardial salvage might be possible.

Unlike neutrophils which are part of the body's innate immunity system responsible for rapid nonspecific defense, lymphocytes belong to the adaptive immunity system responsible for a slower but more specific defense. The lymphocyte-to-CRP (L-C) ratio has been proposed as a quantitative biomarker to assess the specific immunological responses to systemic inflammation in several types of cancer.[19,20] A lower L-C ratio is caused by a decrease in the lymphocyte level and/or an increase in the CRP level, and hence, it reflects an impairment in specific immunological response, which favours inflammatory progression and worse clinical outcome. The L-C ratio has been recently shown to have a useful prognostic value in COVID-19 patients, since SARS-CoV-2 infection also triggers a systemic inflammatory response.[21] A lower L-C ratio in the COVID-19 patients is associated with a higher likelihood of in-hospital mortality.[22] Our data reveals that the COVID-19 patients with ACI had a significantly lower L-C ratio compared to the patients without ACI (0.017 versus 0.058 respectively, $p < 0.05$), further demonstrating the heart injury in some of our COVID-19 patients could be due to the failure of specific immunological response to the viral infection.

Our findings revealed a poor correlation (both linear and non-linear) between the extent of lung injury manifested in NCCT and the arterial blood oxygen level, and the latter was not statistically different between the ACI and non-ACI patient groups. However, cardiac tissue hypoxia could not be completely ruled out based on these findings since the more specific tissue perfusion / hypoxia imaging test was not performed to rule-in or rule-out cardiac hypoxia. The findings of this retrospective study merely suggested that hypoxia precipitated directly by the lung injury was likely not a main contributor of the heart injury at this phase of the disease, and did not exclude the possibility of low oxygen delivery to cardiac tissue as a result of other factors such as reduced myocardial perfusion as suggested by previous studies.[23]

There are several study limitations that should be addressed. First, the diagnostic values of the NCCT-derived metrics for detecting ACI in COVID-19 patients could be affected by other co-existing physiological conditions. Among our COVID-19 patients who did not have ACI, those with diabetes had a lower RVNP level and a higher level of RVMAP, RVSAP and CRP in comparison to the patients without diabetes. A similar trend was also observed in the patients with ACI and hypertension versus those with ACI but without hypertension (Table 3). These findings were in contrast to those of our COVID-19 patients with ACI, whose CRP and normal / abnormal lung tissue volumes were relatively unchanged regardless of the status of hypertension and diabetes. Due to the lack of comprehensive clinical information and the relatively small sample size, the effect of comorbidities could not be fully evaluated in this study.

Second, ACI was diagnosed with high-sensitivity troponin I measurement at a single time point only. It would have been more informative regarding the temporal progression of cardiac injury if the troponin I measurements were taken at multiple time points, from which the diagnostic value of NCCT as a function of time post infection could be assessed more thoroughly. Third, functional cardiac imaging was not acquired and therefore the type and extent of cardiac injury could not be specified.[24] Despite a number of study limitations, the results of this study shed light on the usefulness of non-contrast chest CT findings for predicting cardiac injury during the acute phase of SARS-coV-2 infection, which may facilitate the development of a prognostic model of COVID-19 related cardiac damage with AI-based algorithms. The study findings also indicated that there may exist a narrow time window during which patient treatments can be tailored according to the NCCT and biomarker findings to optimize the chance of myocardial salvage.

In conclusion, the normal and abnormal lung parenchyma volumes delineated from NCCT chest images were statistically signficiant predictors of ACI in COVID-19 patients within approximately two weeks after SARS-CoV-2 infection. The conjunctional use of the NCCT-derived parameter and immunological (lymphocytes) / inflammatory (CRP) markers yielded the highest diagnostic value. These findings may be useful to inform appropriate treatment strategy for COVID-19 patients to minimize the damage in the heart when the more specific functional cardiac imaging is unavailable during the initial diagnostic procedure.

Table 3
Comparison of the four significant predictors of ACI in COVID-19 patients with and without hypertension and diabetes. * denotes statistical difference ($p < 0.05$) from the "with hypertension" group. † denotes statistical difference ($p < 0.05$) from the "with diabetes" group ($p < 0.05$).

	LPV-N (%)	LPV-MA (%)	LVP-SA (%)	CRP (mg/L)
COVID-19 patients with ACI				
with hypertension	65.25 ± 2.66	16.82 ± 2.20	1.88 ± 0.41	60.33 ± 13.37
without hypertension	60.71 ± 1.75	19.03 ± 1.31	3.68 ± 0.48 *	63.81 ± 7.76
with diabetes	61.08 ± 2.05	20.00 ± 1.71	3.87 ± 0.68	71.09 ± 10.74
without diabetes	62.27 ± 2.01	17.64 ± 1.46	2.88 ± 0.45	58.44 ± 8.50
COVID-19 patients without ACI				
with hypertension	61.28 ± 4.86	19.92 ± 3.78	2.47 ± 0.91	36.97 ± 15.80
without hypertension	73.33 ± 1.40 *	11.50 ± 1.02 *	1.25 ± 0.17 *	22.48 ± 4.81
with diabetes	65.58 ± 3.11	16.58 ± 2.59	1.75 ± 0.34	59.25 ± 13.91
without diabetes	73.56 ± 1.60 †	11.46 ± 1.12 †	1.32 ± 0.25	12.68 ± 2.57 †

Declaration of Competing Interest

The authors declare that they have no known competing financial interests or personal relationships that could have appeared to influence the work reported in this paper.

Acknowledgements

The authors sincerely thank AnalyzeDirect Inc. (Overland Park, Kansas, United States) for providing the Analyze software for analyzing the CT images presented in this study, and the funding support from the Natural Sciences and Engineering Research Council of Canada (A So is the recipient of NSERC Discovery Grant RGPIN-2016-06565).

References

[1] M.D. Solomon, E.J. McNulty, J.S. Rana, T.K. Leong, C. Lee, S.-H. Sung, A. P. Ambrosy, S. Sidney, A.S. Go, The Covid-19 Pandemic and the Incidence of Acute Myocardial Infarction, N. Engl. J. Med. 383 (7) (2020) 691–693.
[2] S. Bangalore, A. Sharma, A. Slotwiner, L. Yatskar, R. Harari, B. Shah, H. Ibrahim, G. H. Friedman, C. Thompson, C.L. Alviar, H.L. Chadow, G.I. Fishman, H.R. Reynolds, N. Keller, J.S. Hochman, ST-Segment Elevation in Patients with Covid-19 - A Case Series, N. Engl. J. Med. 382 (25) (2020) 2478–2480.
[3] B. Cosyns, S. Lochy, M.L. Luchian, A. Gimelli, G. Pontone, S.D. Allard, et al., The role of cardiovascular imaging for myocardial injury in hospitalized COVID-19 patients, N. Engl. J. Med. 382 (25) (2020) 2478–2480.
[4] J.P. Lang, X. Wang, F.A. Moura, H.K. Siddiqi, D.A. Morrow, E.A. Bohula, A current review of COVID-19 for the cardiovascular specialist [published online ahead of print, 2020 May 3], Am. Heart J. 226 (2020) 29–44.
[5] M. Bansal, Cardiovascular disease and COVID-19, Diab. Metab. Syndr. 14 (3) (2020) 247–250.
[6] T.J. Guzik, S.A. Mohiddin, A. Dimarco, V. Patel, K. Savvatis, F.M. Marelli-Berg, et al., COVID-19 and the cardiovascular system: implications for risk assessment, diagnosis, and treatment options, Cardiovasc. Res. 116 (10) (2020) 1666–1687.
[7] S. Shi, M. Qin, Y. Cai, T. Liu, B. Shen, F. Yang, S. Cao, X. Liu, Y. Xiang, Q. Zhao, H. Huang, B. Yang, C. Huang, Characteristics and clinical significance of myocardial injury in patients with severe coronavirus disease 2019, Eur. Heart J. 41 (22) (2020) 2070–2079.
[8] T. Guo, Y. Fan, M. Chen, X. Wu, L. Zhang, T. He, H. Wang, J. Wan, X. Wang, Z. Lu, Cardiovascular Implications of Fatal Outcomes of Patients With Coronavirus Disease 2019 (COVID-19), JAMA Cardiol. 5 (7) (2020) 811–818.
[9] S. Agewall, E. Giannitsis, T. Jernberg, H. Katus, Troponin elevation in coronary vs. non-coronary disease, Eur. Heart J. 32 (4) (2011) 404–411.
[10] A. Bularga, K.K. Lee, S. Stewart, A.V. Ferry, A.R. Chapman, L. Marshall, F. E. Strachan, A. Cruickshank, D. Maguire, C. Berry, I. Findlay, A.S.V. Shah, D. E. Newby, N.L. Mills, A. Anand, High-Sensitivity Troponin and the Application of Risk Stratification Thresholds in Patients With Suspected Acute Coronary Syndrome, Circulation 140 (19) (2019) 1557–1568.

[11] B.M. Henry, G. Aggarwal, J. Wong, S. Benoit, J. Vikse, M. Plebani, G. Lippi, Lactate dehydrogenase levels predict coronavirus disease 2019 (COVID-19) severity and mortality: A pooled analysis, Am. J. Emerg. Med. 38 (9) (2020) 1722–1726.

[12] L. Gattinoni, D. Chiumello, P. Caironi, M. Busana, F. Romitti, L. Brazzi, L. Camporota, COVID-19 pneumonia: different respiratory treatments for different phenotypes? Intensive Care Med. 46 (6) (2020) 1099–1102.

[13] N.R. Sproston, J.J. Ashworth, Role of C-Reactive Protein at Sites of Inflammation and Infection, Front. Immunol. 9 (2018) 754.

[14] Y.-Y. Luan, Y.-M. Yao, The Clinical Significance and Potential Role of C-Reactive Protein in Chronic inflammatory and neurodegenerative diseases, Front. Immunol. 9 (2018) 1302.

[15] D.L. Longo, D.C. Fajgenbaum, C.H. June, Cytokine Storm, N. Engl. J. Med. 383 (23) (2020) 2255–2273.

[16] G. Chen, D. Wu, W. Guo, Y. Cao, D. Huang, H. Wang, et al., Clinical and immunologic features in severe and moderate Coronavirus Disease 2019, J. Clin. Invest. 130 (2020) 2620–2629.

[17] D. Sun, H. Li, X.-X. Lu, H. Xiao, J. Ren, F.-R. Zhang, Z.-S. Liu, Clinical features of severe pediatric patients with coronavirus disease 2019 in Wuhan: a single center's observational study, World J. Pediatr. 16 (3) (2020) 251–259.

[18] N. Ali, Elevated level of C-reactive protein may be an early marker to predict risk for severity of COVID-19, J. Med. Virol. 92 (11) (2020) 2409–2411.

[19] Y. Okugawa, Y. Toiyama, A. Yamamoto, T. Shigemori, T. Ichikawa, C. Yin, A. Suzuki, H. Fujikawa, H. Yasuda, J. Hiro, S. Yoshiyama, M. Ohi, T. Araki, D. C. McMillan, M. Kusunoki, Lymphocyte-to-C-reactive protein ratio and score are clinically feasible nutrition-inflammation markers of outcome in patients with gastric cancer, Clin. Nutr. 39 (4) (2020) 1209–1217.

[20] Y. Okugawa, Y. Toiyama, A. Yamamoto, T. Shigemori, S. Ide, T. Kitajima, H. Fujikawa, H. Yasuda, J. Hiro, S. Yoshiyama, T. Yokoe, S. Saigusa, K. Tanaka, Y. Shirai, M. Kobayashi, M. Ohi, T. Araki, D.C. McMillan, C. Miki, A. Goel, M. Kusunoki, Lymphocyte-C-reactive protein ratio as promising new marker for predicting surgical and oncological outcomes in colorectal cancer, Ann. Surg. 272 (2) (2020) 342–351.

[21] W. Ullah, B. Basyal, S. Tariq, T. Almas, R. Saeed, S. Roomi, S. Haq, J. Madara, M. Boigon, D.C. Haas, D.L. Fischman, Lymphocyte-to-C-Reactive Protein Ratio: A Novel Predictor of Adverse Outcomes in COVID-19, J. Clin. Med. Res. 12 (7) (2020) 415–422.

[22] Y. Gao, T. Li, M. Han, X. Li, D. Wu, Y. Xu, Y. Zhu, Y. Liu, X. Wang, L. Wang, Diagnostic utility of clinical laboratory data determinations for patients with the severe COVID-19, J. Med. Virol. 92 (7) (2020) 791–796.

[23] T.R. Porter, K. Costello, J. Olson, F. Xie, J. Lindner, Detection of lung and myocardial perfusion abnormalities in acute COVID-19 infection with bedside ultrasound, J. Am. Coll. Cardiol. 77 (18) (2021) 1299, https://doi.org/10.1016/S0735-1097(21)02657-7.

[24] C. Basso, O. Leone, S. Rizzo, M. De Gaspari, A.C. van der Wal, M.C. Aubry, M. C. Bois, P.T. Lin, J.J. Maleszewski, J.R. Stone, Pathological features of COVID-19-associated myocardial injury: a multicentre cardiovascular pathology study, Eur. Heart J. 41 (39) (2020) 3827–3835.

[25] A. So, Y. Imai, B. Nett, J. Jackson, L. Nett, J. Hsieh, G. Wisenberg, P. Teefy, A. Yadegari, A. Islam, T.-Y. Lee, Technical Note: Evaluation of a 160-mm/256-row CT scanner for whole-heart quantitative myocardial perfusion imaging, Med. Phys. 43 (8Part1) (2016) 4821–4832.

[26] J.E. McDonough, L. Knudsen, A.C. Wright, W.M. Elliott, M. Ochs, J.C. Hogg, Regional differences in alveolar density in the human lung are related to lung height, J. Appl. Physiol. 118 (2015) 1429–1434.